Comprehensive Quantum Calculation of the First Dielectric Virial Coefficient of Water

Giovanni Garberoglio,[1, a)] Chiara Lissoni,[2, b)] Luca Spagnoli,[2, b)] and Allan H. Harvey[3, c)]

[1)] *European Centre for Theoretical Studies in Nuclear Physics and Related Areas (ECT*), Fondazione Bruno Kessler, Trento I-38123, Italy.*

[2)] *Physics Department, University of Trento, Trento I-38123, Italy.*

[3)] *Applied Chemicals and Materials Division, National Institute of Standards and Technology, Boulder, CO 80305, USA.*

We present a complete calculation, fully accounting for quantum effects and for molecular flexibility, of the first dielectric virial coefficient of water and its isotopologues. The contribution of the electronic polarizability is computed from a state-of-the-art intramolecular potential and polarizability surface from the literature, and its small temperature dependence is quantified. The dipolar polarizability is calculated in a similar manner with an accurate literature dipole-moment surface; it differs from the classical result both due to the different molecular geometries sampled at different temperatures and due to the quantization of rotation. We calculate the dipolar contribution independently from spectroscopic information in the HITRAN2020 database and find that the two methods yield consistent results. The resulting first dielectric virial coefficient provides a complete description of the dielectric constant at low density that can be used in humidity metrology and as a boundary condition for new formulations for the static dielectric constant of water and heavy water.

I. INTRODUCTION

Water is crucial in many scientific and industrial contexts. Measurement of the water content of a gas (*i.e.*, humidity) is needed in studies of the atmosphere related to weather and climate processes, but obtaining accurate, fast, and reproducible measurements is challenging. There are also industrial contexts where knowledge of water content is important; an example is natural gas transportation where water can freeze out as ice or form hydrates, both of which are undesirable and potentially dangerous.

One technology that has been proposed for humidity metrology is measurement of the static dielectric constant. Because the molecules in dry air (and, for the most part, in natural gas) are nonpolar, the presence of highly polar water molecules can have a significant effect on the dielectric constant, even at low concentrations. After some preliminary exploration of this approach at the National Institute of Standards and Technology (NIST),[1–3] more fully developed apparatus for measuring this effect was described by Cuccaro *et al.*[4] for water in air and nitrogen and by Gavioso *et al.*[5] for water in methane and natural gas. To apply such measurements in metrology, it is necessary to have an accurate expression for the contribution of water molecules to the static dielectric constant.

The dielectric constant of pure water is of major scientific importance in its own right; it plays a central role in modeling aqueous electrolyte thermodynamics and electrochemical reactions not only in the liquid phase but also at vapor and supercritical conditions with gas-like densities. The International Association for the Properties of Water and Steam (IAPWS) has developed a standard formulation for the static dielectric constant of ordinary water from zero to liquid-like densities,[6] but several deficiencies in this formulation have been noted,[7] including its behavior at low density. Better theoretical knowledge of the dielectric behavior of low-density water would provide an important boundary condition for an improved formulation.

Heavy water (D_2O) is also used in studies of electrolyte solutions, for example in comparison with light water to elucidate the details of ion hydration or to study electrochemistry of species relevant to heavy-water reactors.[8] Knowledge of the dielectric constant is again needed, but efforts to develop a formulation for the static dielectric constant of D_2O are hampered by a lack of experimental data.[9] As with H_2O, a low-density boundary condition would aid these important modeling efforts.

For a low-density gas with a dipole moment, the well-known classical relationship of the static dielectric constant ε to the static isotropic electronic polarizability α and the squared magnitude of the molecular dipole moment μ^2 of the gas constituent is given by the Debye–Langevin modification of the Clausius–Mossotti expression (CMDL):

$$\frac{\varepsilon - 1}{\varepsilon + 2} = \frac{4\pi}{3} N_A \rho \left(\alpha + \frac{\mu^2}{3 k_B T} \right), \qquad (1)$$

where N_A is the Avogadro constant, ρ is the molar density, and k_B is the Boltzmann constant. The first dielectric virial coefficient A_ε is defined as the low-density limit of the proportionality constant between the density and the Clausius–Mossotti quotient:

$$A_\varepsilon \equiv \lim_{\rho \to 0} \frac{1}{\rho} \frac{\varepsilon - 1}{\varepsilon + 2}. \qquad (2)$$

[a)] Electronic mail: garberoglio@ectstar.eu

[b)] These authors contributed equally.

[c)] Electronic mail: allan.harvey@nist.gov

For low-density gas mixtures, the left-hand side of Eq. (1) is simply the sum of ρA_ε of each pure component.

One might think that Eq. (1) provides a simple route to the calculation of A_ε for water, and therefore to humidity metrology. The isotropic electronic polarizability of the water molecule in the ground rovibrational state has been calculated by *ab initio* quantum mechanics,[10] and the result is in good agreement with extrapolation of gas-phase refractivity measurements to the static limit.[11,12] The dipole moment of the H_2O molecule in the rovibrational ground state has been measured to a relative uncertainty of 5×10^{-5}.[13]

There are, however, several ways in which the classical Eq. (1) is oversimplified and slightly inaccurate. The purpose of this paper is to provide a rigorous accounting of all effects on A_ε, all of which involve quantum mechanics in one form or another.

First, the quantization of rotation means that the classical expression is inexact. A first-order correction for this quantum effect was first derived for rigid linear molecules by MacRury and Steele,[14] and was generalized to rigid nonlinear molecules by Gray *et al.*[15]

Second, molecules are not rigid objects, and hence the electronic polarizability has a small temperature dependence. Only at 0 K does it assume the ground-state value; at higher temperatures other rovibrational states are occupied, each of which has a slightly different electronic polarizability.

Third, there is a similar effect for the dipole moment. The excited rovibrational states populated at finite temperatures have somewhat different dipole moments than the ground-state value. Additionally, the proper quantum mechanical derivation of the expression for the first dielectric virial coefficient shows that the generalizaton of Eq. (1) does not simply involve the average value of the dipole moment.

In this paper, we will discuss in detail how Eq. (1) is modified by quantum mechanical effects involving the rovibrational states of the water molecule. Additionally, we will provide the first fully quantum calculation of the first dielectric coefficient A_ε of Eq. (2), discussing in detail the various quantum effects that one might expect for H_2O and its isotopologues due to their small moments of inertia and molecular flexibility.

We are not aware of any application for our results below the frost-point temperatures of gases with trace humidity levels (perhaps ~170 K). We perform computations down to 50 K for completeness, because the physical effects are interesting, and because for some quantities an alternative approach that has very low uncertainty below about 150 K allows us to validate our calculations.

II. THE FIRST DIELECTRIC VIRIAL COEFFICIENT OF A QUANTUM POLAR MOLECULE

The statistical derivation of the CMDL equation shows that the dielectric constant of a gas depends on the derivative of the polarization density $P(F)$ in an external electric field F evaluated at zero field,[15–17]

$$\frac{\varepsilon - 1}{\varepsilon + 2} = \frac{4\pi}{3} \left. \frac{\mathrm{d}P(F)}{\mathrm{d}F} \right|_{F=0} \simeq A_\varepsilon \rho = \frac{4\pi}{3} \left. \frac{\mathrm{d}p(F)}{\mathrm{d}F} \right|_{F=0} \rho N_A, \tag{3}$$

where in the right-hand side we have expanded $P(F)$ to first order as a function of the molar density ρ,[17] that is $P(F) = \rho N_A p(F)$ where $p(F)$ is the dipole moment of an isolated molecule in the external field F. The quantity A_ε is the first dielectric virial coefficient.

The dipole moment of a molecule in thermodynamic equilibrium at temperature T in an electric field is given by the expectation value

$$p(F) = \frac{\mathrm{Tr}\left[(\mathbf{m}\cdot\mathbf{e} + \mathbf{e}\cdot\boldsymbol{\alpha}\cdot\mathbf{e}F)\,\exp\left(-\beta H(F)\right)\right]}{\mathrm{Tr}\left[e^{-\beta H(F)}\right]} \tag{4}$$

$$H(F) = H_0 - F\,\mathbf{m}\cdot\mathbf{e} - \frac{F^2}{2}\,\mathbf{e}\cdot\boldsymbol{\alpha}\cdot\mathbf{e}, \tag{5}$$

where H_0 is the Hamiltonian of the free molecule, $\beta = (k_B T)^{-1}$, $\mathbf{e}$ is a unit vector in the direction of the externally applied electric field of magnitude F, $\boldsymbol{\alpha}$ is the molecular electronic polarizability tensor, and $\mathbf{m}$ is the molecular dipole moment. Notice that, in general, both the dipole moment $\mathbf{m}$ and the electronic polarizability tensor $\boldsymbol{\alpha}$ depend on the specific molecular orientation and configuration which, in the case of water, is determined by 6 degrees of freedom. Usually, these are given by three Euler angles defining the relation between the molecule-fixed and the the laboratory-fixed coordinate system,[18] the lengths r_1 and r_2 of the two O–H bonds, and the angle θ between their directions. The denominator in Eq. (4) is the partition function of a single molecule, and will be denoted by $Q_1(\beta, F)$.

A. Classical and semiclassical limit for rigid rotors

The evaluation of the derivative at zero external field appearing in equations (3), (4), and (5) can be performed explicitly. Its derivation is reported in the Supplementary Material and it shows that, in general, the first dielectric virial coefficient has two contributions,

$$A_\varepsilon = \frac{4\pi}{3} N_A \left(\alpha_{\mathrm{el}} + \alpha_{\mathrm{dip}}\right), \tag{6}$$

where the first depends on the electronic polarizability surface $\boldsymbol{\alpha}$, while the second depends on the dipole-moment surface $\mathbf{m}$. In the classical limit, one recovers Eq. (1)

$$A_\varepsilon^{(\mathrm{cl})} = \frac{4\pi}{3} N_A \left\langle \alpha_{\mathrm{el}} + \frac{\beta|\mathbf{m}|^2}{3} \right\rangle, \tag{7}$$

where the average $\langle\cdots\rangle$ is over the internal configurations of the molecule; this is the result quoted in Ref. 14 and shows how to interpret the quantities α and μ^2 in Eq. (1),

which are the values of the electronic polarizability and the squared magnitude of the dipole moment at the assumed rigid configuration of water. In a simple classical rigid model of water (*e.g.*, when the bond lengths r_1 and r_2 and the angle θ are fixed at their ground-state values[19]), the contribution to A_ε from the dipole moment is $A_\varepsilon^{(\text{dip,cl})} \sim 70.2$ cm^3/mol at $T = 300$ K, whereas that from the electronic polarizability tensor is on the order of $A_\varepsilon^{(\text{el,cl})} \sim 3.7$ cm^3/mol.

Semiclassical corrections to the dipolar contribution in Eq. (7) have been derived in Ref. 15, and are given by

$$\frac{\Delta A_\varepsilon^{(\text{dip,semi})}}{A_\varepsilon^{(\text{dip,cl})}} = -\frac{\beta\hbar^2}{12|\mathbf{m}|^2}\left(\frac{m_y^2 + m_z^2}{I_x} + \frac{m_z^2 + m_x^2}{I_y} + \frac{m_x^2 + m_y^2}{I_z}\right), \quad (8)$$

where I_i are the principal moments of inertia of the molecule and m_i are the components of the dipole moment along the principal axis. For water at 300 K, the semiclassical correction of Eq. (8) is $A_\varepsilon^{(\text{semi})} = -2.0$ cm^3/mol, which in relative terms is roughly 3% of the dipolar contribution.

B. Quantum statistics

In the general case, one has to be careful in performing the derivative with respect to F in Eq. (3), due to the presence of non-commuting operators. Denoting by $|i\rangle$ a complete set of molecular rovibrational quantum states and by E_i the corresponding energies, the fully quantum expressions for the two terms in Eq. (6) are (see the Supplementary Material for the derivation)

$$\alpha_{\text{el}}(T) = \frac{1}{Q_1(\beta, 0)}\sum_i \frac{\langle i|\text{Tr}(\boldsymbol{\alpha})|i\rangle}{3}\, e^{-\beta E_i}, \quad (9)$$

$$\alpha_{\text{dip}}(T) = \frac{1}{Q_1(\beta, 0)}\sum_{i \neq j} |\langle i|\mathbf{m} \cdot \mathbf{e}|j\rangle|^2 \frac{e^{-\beta E_i} - e^{-\beta E_j}}{E_j - E_i}. \quad (10)$$

The quantum mechanical formula for α_{dip} was first derived by Illinger and Smyth.[20] In general, a molecular eigenstate $|i\rangle$ is characterized by a set of rotational and vibrational quantum numbers and hence one can split the sum in Eq. (10) into two contributions: the first corresponds to those $i \leftrightarrow j$ transitions where the vibrational state changes, resulting in the so-called *vibrational polarizability*. The sum over the remaining transitions, which have the same vibrational quantum numbers, is called the *rotational polarizability*.[21]

In the $T \to 0$ limit, the electronic polarizability (9) becomes just an average over the ground rovibrational state $|0\rangle$, that is

$$\alpha_{\text{el}}^0 = \frac{1}{3}\langle 0|\text{Tr}(\boldsymbol{\alpha})|0\rangle, \quad (11)$$

whereas the dipolar polarizability becomes[21]

$$\alpha_{\text{dip}}^0 = 2\sum_{j \neq 0}\frac{|\langle 0|\mathbf{m} \cdot \mathbf{e}|j\rangle|^2}{E_j - E_0} = \frac{2}{3}\sum_{j \neq 0}\frac{|\langle 0|\mathbf{m}|j\rangle|^2}{E_j - E_0}, \quad (12)$$

where we have used rotational invariance to substitute $\mathbf{e} \cdot \boldsymbol{\alpha} \cdot \mathbf{e} = \text{Tr}(\boldsymbol{\alpha})/3$ and $|\langle i|\mathbf{m} \cdot \mathbf{e}|j\rangle|^2 = |\langle i|\mathbf{m}|j\rangle|^2/3$.

In the high-temperature (classical) limit, $T \to \infty$, one can write

$$e^{-\beta E_i} - e^{-\beta E_j} \simeq e^{-\beta E_i}\beta(E_j - E_i), \quad (13)$$

and Eq. (10) becomes

$$\alpha_{\text{dip}}^{\text{class}}(T) = \frac{\beta}{3}\frac{\sum_i \langle i||\mathbf{m}|^2|i\rangle e^{-\beta E_i}}{Q_1(\beta, 0)}, \quad (14)$$

which can be seen as a generalization of the classical expression (7) where the square of the permanent dipole is replaced by its quantum thermal average, which depends only on the diagonal matrix elements of the corresponding operator. In general, however, the dipolar contribution to the first dielectric virial coefficient depends on all the matrix elements of the dipole moment, as evidenced by Eq. (10).

III. DIPOLAR POLARIZABILITY FROM SPECTROSCOPY

The dipolar polarizability (10) depends on the squared matrix elements of the dipole operator $\mathbf{m}$, which is the same operator that determines the Einstein coefficient associated with an electromagnetic transition between states of energy E_i and E_j.[22] These coefficients, or equivalently the line intensities, of several thousands of transitions are available in the HITRAN2020 database[23] for many water isotopologues, as well as other molecules. This paves the way to an experimental determination of the dipolar polarizability from spectroscopic data.

To this end, let us rewrite Eq. (10) according to the following considerations: first of all, we notice that the quantity to be summed is invariant under the exchange $i \leftrightarrow j$. Hence, the dipolar polarizability is given by twice the sum performed over those states for which $E_j > E_i$. Second, there might be degeneracies among the energy levels, so let us denote by d_i the number of states having energy E_i; in the case of water $d_i = (2J + 1)g_i$ where J is the angular momentum of state i and g_i is its nuclear-spin degeneracy. A general state $|i\rangle$ can then be labeled by its energy E_i and an integer ξ running between 1 and d_i. Finally, let us define the average dipole matrix element squared between levels with energy E_i and E_j as

$$M_{ij} = \frac{1}{d_i d_j}\sum_{\xi=1}^{d_i}\sum_{\eta=1}^{d_j}|\langle E_i, \xi|\mathbf{m} \cdot \mathbf{e}|E_j, \eta\rangle|^2, \quad (15)$$

and the transition frequency $\omega_{ij} = (E_j - E_i)/\hbar$. With these definitions, we can write the dipolar polarizability

as

$$\alpha_{\text{dip}}(T) = \frac{2}{Q_1(\beta)} \sum_{E_j > E_i} \frac{d_i d_j M_{ij}}{\hbar \omega_{ij}} e^{-\beta E_i} \left(1 - e^{-\beta \hbar \omega_{ij}} \right).$$

(16)

On the other hand, the spectral line intensities S_{ij} for the transitions between molecular levels of energy E_i and E_j reported in the HITRAN2020 database are given by (in our notation)[24,25]

$$S_{ij} = \frac{2\pi}{\hbar c} I_A \omega_{ij} d_i d_j M_{ij} \frac{e^{-\beta_{\text{R}} E_i} \left(1 - e^{-\beta_{\text{R}} \hbar \omega_{ij}} \right)}{Q_1(\beta_{\text{R}})},$$

(17)

where c is the speed of light, I_A is the isotopic abundance of the species under consideration, $\beta_{\text{R}} = (k_{\text{B}} T_{\text{R}})^{-1}$, and $T_{\text{R}} = 296$ K is a reference temperature. Consequently, one can write

$$\alpha_{\text{dip}}(T) = \frac{c}{\pi I_A} \sum_{E_j > E_i} \frac{S_{ij}}{\omega_{ij}^2} \frac{Q_1(\beta_{\text{R}})}{e^{-\beta_{\text{R}} E_i} \left(1 - e^{-\beta_{\text{R}} \hbar \omega_{ij}} \right)} \times$$
$$\frac{e^{-\beta E_i} \left(1 - e^{-\beta \hbar \omega_{ij}} \right)}{Q_1(\beta)},$$

(18)

which enables the calculation of the dipolar polarizability based on the quantities S_{ij}, ω_{ij}, E_i, $Q_1(\beta)$, that are all reported the HITRAN2020 database. Since the HITRAN2020 database also reports quantum numbers for the upper and lower states of the transitions, the calculation of the vibrational and rotational contributions to the dipolar polarizability using Eq. (18) is straightforward.

The HITRAN2020 database also reports the uncertainty associated with the line intensities S_{ij}; we have used this information to propagate it to the uncertainty of $A_\varepsilon^{(\text{dip})}$ using Eq. (18). In those cases where HITRAN2020 reported a range for the uncertainty, we made the conservative choice of taking the highest value and considering it to be a standard uncertainty.

We note that any errors in the HITRAN-calculated values will be highly correlated, because the same data for lines and intensities are used at each temperature (just weighted differently). This makes the scatter of the results calculated from HITRAN2020 much less than the uncertainties of those results.

IV. AB INITIO CALCULATION OF THE FIRST DIELECTRIC VIRIAL COEFFICIENT

The quantities $\alpha_{\text{el}}(T)$ and $\alpha_{\text{dip}}(T)$ can be computed from the knowledge of the intramolecular potential, the trace of the polarizability $\alpha(\mathbf{X}) = \text{Tr}(\boldsymbol{\alpha})$, and the dipole moment $\mathbf{m}(\mathbf{X})$, where $\mathbf{X}$ denotes a set of intramolecular coordinates (e.g., the two bond lengths and the HOH angle). All of these quantities are available from ab initio electronic structure calculations. In particular, we used the recent PES15K[26] potential-energy surface to compute the intramolecular potential, the dipole-moment surface $\mathbf{m}(\mathbf{X})$ CKAPTEN from Ref. 27, and the isotropic

electronic polarizability $\alpha(\mathbf{X})$ from Ref. 10. In Ref. 10, the authors provide a fitting function based on extensive calculations of the polarizability for many molecular configurations (the DPS-H$_2$O-3K database), solving the electronic structure at the CCSDT/daTZ level of theory. In addition, they perfomed a few evaluations of the polarizability surface at a more accurate level of theory (CCSDT/daQZ + $\Delta\alpha_{\text{basis}}$ + $\Delta\alpha_{\text{core}}$). The values obtained in this case are much more accurate for configurations close to the equilibrium configuration of water. Therefore, we slightly changed their parametrization of the polarizability surface (from their Table II[10]) in order to obtain more accurate values around the equilibrium geometry. In practice, we changed the first line of their Table II (corresponding to $(ijk) = (000)$) to the values reported in their Table III, that is $\alpha_{xx} = 9.8744$, $\alpha_{yy} = 9.2233$, and $\alpha_{zz} = 9.5190$ (in atomic units). This corresponds to a rigid shift of the isotropic part of the CKAPTEN polarizability surface by $\Delta\alpha_{\text{iso}} = -0.039133$ atomic units, which in relative terms is approximately 0.4%.

There are two main ways to compute the first dielectric virial coefficient for water. The first is to diagonalize the Schrödinger equation for the nuclear motion of the water molecule, compute the temperature-dependent electronic polarizability of Eq. (9) and the dipolar polarizability of Eq. (10), and obtain the first dielectic virial coefficient from Eq. (6). Although there are efficient approaches to solve the quantum-mechanical three-body problem and obtain the rovibrational eigenstates of water molecules, a complete diagonalization of the intramolecular Hamiltonian becomes progressively more difficult for molecules with a larger number of atoms. We will show in the following how the two temperature-dependent contributions to $A_\varepsilon(T)$ can be obtained from a path-integral approach, which has a much more favorable computational scaling for polyatomic molecules.

A. The discrete variable representation approach

In the case of water or other triatomic molecules, it is convenient to use the form of the three-body Hamiltonian in the molecule-fixed frame derived by Sutcliffe and Tennyson using Jacobi coordinates.[28] In this approach, one obtains, for each value of the total molecular angular momentum J, a vibrational Hamiltonian that depends on three coordinates: the moduli of the two Jacobi vectors, R_1 and R_2, and the value of the angle between them, Θ. The full rovibrational spectrum of water can be obtained by diagonalizing the vibrational Hamiltonian for progressively larger values of the molecular angular momentum J. The Hamiltonian is conveniently written using the so-called Discrete Variable Representation (DVR),[29–31] which has been used in many investigations of water properties.[32,33]

In practice, the rovibrational wavefunction is written

as

$$\Psi_{J\nu mI}(q,\Omega,I) =$$
$$\sqrt{\frac{2J+1}{8\pi^2}} \sum_{k=-J}^{J} \psi_{J\nu}(q,k) D_{mk}^{J}(\Omega)\chi(\mathcal{I}_{J\nu},I), \quad (19)$$

where $q = (R_1, R_2, \Theta)$ denotes the molecular vibrational coordinates, $\psi_{J\nu}(q,k)$ are the eigenfunctions of the rovibrational Hamiltonian in the molecule-fixed frame for a given value of J, $D_{mk}^{J}(\Omega)$ are Wigner rotation matrices from the molecule-fixed to the laboratory-fixed frames, and $\chi(\mathcal{I}_{J\nu},I)$ denotes the wavefunction of nuclear spins, with total spin $\mathcal{I}_{J\nu}$ and projection I along the laboratory Z axis. In the case of water molecules with two identical hydrogen isotopes, the overall wavefunction in Eq. (19) must have a specific symmetry upon exchange of the two hydrogens, reflecting their fermionic (H or T, antisymmetric wavefunction) or bosonic (D, symmetric wavefunction) nature. The need of a well-defined exchange symmetry for the total wavefunction implies that the nuclear-spin state of the two hydrogens depends on exchange symmetry of the rovibrational state $\psi_{J\nu}$.

In the case of two hydrogen atoms (with nuclear spin 1/2), molecular configurations have either $\mathcal{I}_{J\nu} = 0$ (para-water) or $\mathcal{I}_{J\nu} = 1$ (ortho-water), with multiplicities $g_{\text{para}} = 1$ and $g_{\text{ortho}} = 3$, respectively. In the case of two deuterium atoms (with nuclear spin 1), the ortho spin isomer has total spin $\mathcal{I}$ which is either 0 or 2 (that is, degeneracy $g_{\text{ortho}} = 6$) or total spin 1, with degeneracy $g_{\text{para}} = 3$. For the sake of completeness, we recall that nuclear spin degeneracies can also come from the oxygen spin, although in this case they do not depend on the rovibrational state. This is particularly relevant for the ^{17}O oxygen isotope, which has $\mathcal{I} = 5/2$. The other oxygen isotopes have $\mathcal{I} = 0$.

Notice that the energy levels on the molecular Hamiltonian depend only on the quantum numbers J (the total angular momentum), k (the projection of the angular momentum in the molecule-fixed z axis), and ν (that labels the vibrational states obtained for given values of J and k). Rotational invariance implies a $2J+1$ degeneracy on the label m in Eq. (19).

Evaluating the symmetry upon exchange of the wavefunctions $\psi_{J\nu k}(q)$, and hence the degeneracy, is a non-trivial procedure,[34] but this information is already included in the HITRAN2020 database. Given the accuracy of our calculated energy levels (see details of the calculations in section V B 2), we assigned degeneracies by looking at that of the closest energy level, for a given J, among the states present in HITRAN2020. Using the DVR approach, one can compute the electronic and dipolar contribution to the polarizability directly from the quantum mechanical expressions of Eqs. (9) and (10),

respectively. In the first case, one obtains

$$\alpha_{\text{el}}(T) = \sum_{J\nu} \frac{g_{J\nu}(2J+1)e^{-\beta E_{J\nu}}}{3\, Q_1(\beta,0)} \langle \psi_{J\nu}|\text{Tr}(\boldsymbol{\alpha})|\psi_{J\nu}\rangle, \quad (20)$$

where $g_{J\nu}$ is the degeneracy of the given rovibrational state and, in the DVR representation, one has

$$\langle \psi_{J\nu}|\text{Tr}(\boldsymbol{\alpha})|\psi_{J\nu}\rangle = \sum_{q,k} |\psi_{J\nu k}(q)|^2 \,\text{Tr}(\boldsymbol{\alpha}(q)), \quad (21)$$

since the trace of the polarizability tensor $\boldsymbol{\alpha}(q)$ is a scalar quantity and a diagonal operator in the DVR representation. Notice that in the case of a rigid model of water, the electronic polarizability (20) does not depend on temperature.

The quantum mechanical expression for $\alpha_{\text{dip}}(T)$ is more complicated, because one needs to evaluate the matrix element of the components of the dipole moment $\mathbf{m}$ in the laboratory-fixed frame using wavefunctions defined in the molecule-fixed frame.[18,32,35] Its derivation is discussed in Appendix A, for both rigid and flexible molecular models.

B. The path-integral approach

A first-principles evaluation of the first dielectric virial coefficient from Eqs. (3)–(5) can also be performed using the path-integral formulation of quantum statistical mechanics.[36] The main advantage of this method is that it works directly in the Cartesian coordinates of all the atoms, and hence one does not need the analytically complicated procedure of separating the center-of-mass, rotational, and vibrational motion as needed for solving the Schrödinger equation.

1. Quantum rigid rotors

In the case of a rigid rotor, α_{el} is a constant and hence easily evaluated. Taking the derivative with respect to F of the first term in Eq. (3) requires some care, because the dipole moment direction in the laboratory reference frame, $\mathbf{m} \cdot \mathbf{e}$ (which will be denoted by m_Z in the following), does not commute with H_0 which, in this case, is the Hamiltonian of a quantum asymmetric rigid rotor. It is convenient to specialize the trace as an integration over all possible orientations of the molecule – which will be denoted by Ω_1 – and at the same time use Trotter's identity to write

$$e^{-\beta H_0 + \beta \mathbf{m}\cdot\mathbf{e}F} \sim \left(e^{-\beta H_0/P}e^{\beta(\mathbf{m}\cdot\mathbf{e})F/P}\right)^P, \quad (22)$$

which becomes an equality for a sufficiently large P. Inserting $P-1$ completeness relations of the form

$$1 = \int |\Omega_k\rangle\langle\Omega_k|\, d\Omega_k,$$

between the P products in Eq. (22), one ends up with the expression

$$A_\varepsilon = \frac{4\pi}{3}\alpha_{\rm el} + \frac{4\pi}{3Q_1}\frac{\partial}{\partial F}\int m_Z(\Omega_1)\prod_{k=1}^{P}\langle\Omega_k|{\rm e}^{-\beta H_0/P}|\Omega_{k+1}\rangle\,{\rm e}^{\beta m_Z(\Omega_{k+1})F/P}\prod_{k=1}^{P}{\rm d}\Omega_k \tag{23}$$

$$= \frac{4\pi}{3}\alpha_{\rm el} + \frac{4\pi}{3Q_1}\int m_Z(\Omega_1)\prod_{k=1}^{P}\langle\Omega_k|{\rm e}^{-\beta H_0/P}|\Omega_{k+1}\rangle\left[\frac{\beta}{P}\sum_{k=1}^{P}m_Z(\Omega_k)\right]\prod_{k=1}^{P}{\rm d}\Omega_k \tag{24}$$

$$= \frac{4\pi}{3}\alpha_{\rm el} + \frac{4\pi\beta}{3Q_1}\int \prod_{k=1}^{P}\langle\Omega_k|{\rm e}^{-\beta H_0/P}|\Omega_{k+1}\rangle\left[\frac{1}{P}\sum_{k=1}^{P}m_Z(\Omega_k)\right]^2\prod_{k=1}^{P}{\rm d}\Omega_k, \tag{25}$$

$$= \frac{4\pi}{3}\alpha_{\rm el} + \frac{4\pi\beta}{9}\left\langle|\overline{\mathbf{m}}|^2\right\rangle, \tag{26}$$

where we have defined $\overline{\mathbf{m}} = \sum_k \mathbf{m}(\Omega_k)/P$. In passing from (24) to (25), we have used the fact that singling out $m_Z(\Omega_1)$ in (23) is an arbitrary choice that we have averaged upon. Notice also that we have defined $\Omega_{P+1} = \Omega_1$. The evaluation of the matrix elements $\langle\Omega_k|{\rm e}^{-\beta H_0/P}|\Omega_{k+1}\rangle$ for a rigid-rotor molecule is discussed in Refs. 37 and 38.

2. Quantum flexible molecules

In dealing with flexible models of water, it is convenient to denote by $\mathbf{X}$ the set of all the coordinates of the three atoms. In this case, A_ε is still given by Eq. (3) where the Hamiltonian H_0 includes the kinetic energy of the three atoms, K, and the intramolecular potential $V_{\rm int}(\mathbf{X})$. Note that both the dipole moment $\mathbf{m}$ and the electronic polarizability tensor $\boldsymbol{\alpha}$ depend on $\mathbf{X}$. The path-integral evaluation of quantities related to flexible molecules has been described in detail in Ref. 39. The main result is that one can map the quantum partition function to a classical partition function where each atom is represented by a ring polymer with P beads. This approach provides an explicit expression of the interaction between consecutive beads (that turns out to be an harmonic potential) and the interaction among the ring polymers, which depends on $V_{\rm int}(\mathbf{X})$. In the case of H_2O or D_2O, one has to consider the indistinguishability between the hydrogen or deuterium atoms within a molecule. Although this can be done in the path-integral approach, it can be shown that exchange effects are important only for temperatures $T \lesssim 50$ K[39] and therefore they will be neglected in this paper.

With a derivation analogous to that performed in the case of rigid rotors, the path-integral expression for A_ε

in the case of a flexible model turns out to be

$$A_\varepsilon = \frac{4\pi}{3}\int\left(\overline{\alpha_{\rm el}} + \frac{\beta}{3}|\overline{\mathbf{m}}|^2\right)\times$$
$$\mathcal{P}(\mathbf{X}_1,\dots,\mathbf{X}_P)\prod_{k=1}^{P}{\rm d}\mathbf{X}_k \tag{27}$$

$$\overline{\alpha_{\rm el}} = \frac{1}{P}\sum_{k=1}^{P}\alpha_{\rm el}(\mathbf{X}_k) \tag{28}$$

$$\overline{\mathbf{m}} = \frac{1}{P}\sum_{k=1}^{P}\mathbf{m}(\mathbf{X}_k) \tag{29}$$

$$\mathcal{P}(\mathbf{X}_1,\dots,\mathbf{X}_P) = \frac{1}{Q_1}\prod_{k=1}^{P}\langle\mathbf{X}_k|{\rm e}^{-\beta T}|\mathbf{X}_{k+1}\rangle\times$$
$$\exp\left(-\frac{\beta}{P}\sum_{k=1}^{P}V_{\rm int}(\mathbf{X}_k)\right), \tag{30}$$

where $\mathcal{P}(\cdots)$ is the probability of finding a specific molecular configuration in the path-integral representation.

The first term in Eq. (27) is the path-integral representation of the electronic contribution to the electronic polarizability of Eq. (9),[21,40] whereas the second term corresponds to the temperature-dependent dipolar polarizability, Eq. (10).

V. NUMERICAL IMPLEMENTATION

A. Quantum rigid rotors

1. Path-integral Monte Carlo

In the case of quantum rigid rotors, our path-integral Monte Carlo (PIMC) simulation followed the procedure outlined in Refs. 37 and 38. We considered the underlying rigid model of water by using the ground-state geometric parameters in Ref. 19 ($r_1 = r_2 = 0.97565$ Å and $\theta = 104.43°$ for H_2O; $r_1 = r_2 = 0.97077$ Å and $\theta = 104.408°$ for D_2O), and those developed in Ref. 41 for $HD^{16}O$ ($r_1 = 0.97126$ Å, $r_2 = 0.96947$ Å, $\theta = 104.01°$), where r_1 and r_2 are the two bondlengths and θ is the bending angle of the water molecule.

We found convergence of the values of the dipolar polarizability using $P = {\rm nint}(5 + 700\ {\rm K}/T)$, where T is the temperature and ${\rm nint}(x)$ denotes the nearest integer to

the number x. We performed 100000 Monte Carlo moves (corresponding to an attempted rotation of a molecule in one of the imaginary-time slices) for equilibration, and we then averaged the values of the dipole moment on 256 independent runs each one sampling 1000 configurations, separated by 50 Monte Carlo moves.

2. Hamiltonian diagonalization

In the case of a rigid water model, the coordinates q in Eq. (19) are fixed, and the wavefunctions are given by

$$\Psi_{J\nu m I}(\Omega, I) = \sqrt{\frac{2J+1}{8\pi^2}} \sum_{k=-J}^{J} \psi_{J\nu k} D_{mk}^{J}(\Omega) \chi(\mathcal{I}_{J\nu}, I). \quad (31)$$

The quantities $\psi_{J\nu k}$ can be obtained by diagonalization of the rigid-rotor Hamiltonian in the molecule-fixed frame, that is

$$H_{\mathrm{R}} = \frac{\hbar^2}{2}\left(\frac{J_a^2}{I_a} + \frac{J_b^2}{I_b} + \frac{J_c^2}{I_c}\right), \quad (32)$$

where J_i are the angular momentum operators in the molecular frame, and $I_a \le I_b \le I_c$ are the principal inertia moments of the molecule.[18] The index ν of the rigid-rotor eigenfunction labels the rotational states of H_{R} for a given total angular momentum J and therefore is an integer between $-J$ and J (inclusive).

In the case of rigid asymmetric rotors, such as water, the eigenfunctions for a given total angular momentum J are usually labeled with the notation $J_{K_a K_c}$ where K_a and K_c denote the absolute value of the projection K of the angular momentum in the molecular frame in the limits $I_b \to I_a < I_c$ (oblate symmetrical top) and $I_a < I_b \to I_c$ (prolate symmetrical top). In both of these limits, K is a good quantum number and states with the same value of $|K|$ are degenerate. The nuclear-spin degeneracy is related to the value of $K_a + K_c$: for $H_2^{16}O$ one has that $g_{J\nu} = 1$ if $K_a + K_c$ is even (para-$H_2^{16}O$), and $g_{J\nu} = 3$ if $K_a + K_c$ is odd (ortho-$H_2^{16}O$), while for $D_2^{16}O$ one has that $g_{J\nu} = 6$ if $K_a + K_c$ is even (ortho-$D_2^{16}O$), and $g_{J\nu} = 3$ if $K_a + K_c$ is odd (para-$D_2^{16}O$).

We performed rigid-model calculations by numerical diagonalization of the Hamiltonian of Eq. (32) up to $J = 40$.

B. Quantum flexible molecules

1. Path-integral Monte Carlo

We checked convergence of various components of the first dielectric virial coefficient with the number of beads P, and we found that it was reached using $P = 70 + \mathrm{nint}(10000\,\mathrm{K}/T)$ for every possible isotopologue. In order to perform PIMC calculations, we developed code based on the hybrid Monte Carlo method[42] to sample molecular configurations according to the probability of Eq. (30). We used 200000 steps for equilibration and then evaluated average values using at least 512 independent runs of 600000 steps, sampling observables every 1000 steps.

2. Discrete Variable Representation

We developed a DVR code in house. $N_r = 28$ and $N_\theta = 28$ basis set points for the radial and angular coordinates, respectively, were sufficient to obtain rovibrational energies within one part in 10^6 from the reference values calculated in Ref. 26 for $J = 0$. Limitations in memory and CPU time available prevented us from computing rovibrational states at angular momenta higher than $J = 19$. Comparison between the partition functions obtained with our approach and the reference ones available in the HITRAN2020 database[23] showed that this limitation results in a systematic uncertainty of at most 0.6% for H_2O at the highest temperature at which we have used this approach, $T = 500$ K. As a further check of our implementation, we computed the average values of the O–H bond-length and H-O-H angle for H_2O and D_2O in the $J = 0$ subspace, and they were found to agree with the results of Ref. 19 to within one part in 10^5.

VI. RESULTS AND DISCUSSION FOR $H_2^{16}O$

In this section, we will discuss in detail our results relative to the most common water isotopologue, $H_2^{16}O$. The results for two other isotopologues, $HD^{16}O$ and $D_2^{16}O$, are reported in the Supplementary Material.

A. Electronic polarizability

Let us begin our discussion by considering the electronic polarizability contribution to the first virial coefficient, that is $\alpha_{\mathrm{el}}(T)$ defined in Eq. (9). As a first approximation, e.g., by using a classical rigid model for the water molecule, it can be calculated as the value of the electronic polarizability surface at the average geometric parameters (distances and angles) of the molecular ground state;[19] in this case one obtains the value $A_\varepsilon^{(\mathrm{el})} = 3.659$ cm^3/mol. However, one should in fact average the value of the electronic polarizability surface over the distribution of configurations sampled by the ground state of the water molecule. This procedure, performed using the DVR ground-state wavefunction, provides $A_\varepsilon^{(\mathrm{el})} = 3.678$ cm^3/mol and shows that a simple classical model underestimates the actual value by −0.5% in the $T \to 0$ limit. Comparing the ground-state averaged value of the electronic polarizability with its value at the

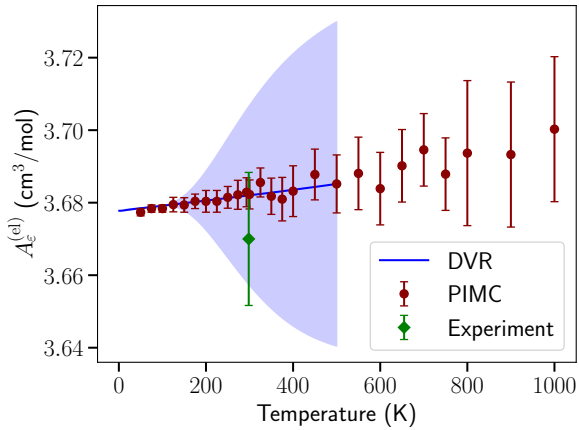FIG. 1. The electronic polarizability contribution to A_ε, $A_\varepsilon^{(el)}$, of $H_2{}^{16}O$ as a function of temperature, obtained from computer simulations. The blue line is the result of our DVR calculations, together with an estimated uncertainty coming from the limited number of angular momenta that have been considered, reported as a blue area. Filled circles are the results of the path-integral simulations and the diamond is the experimental result of Ref. 12, adjusted to zero frequency using the dipole oscillator strength sums of Zeiss and Meath.[43] All uncertainties are reported at the $k = 2$ coverage value and do not include the propagation of the unknown uncertainty of the water electronic polarizability surface.

geometry where the intramolecular potential has its minimum ($r_1 = r_2 = 0.9579$ Å and $\theta = 104.512°$, corresponding to $A_\varepsilon^{(el,min)} = 3.566$ cm^3/mol), one immediately obtains an estimate of the so-called vibrational contribution to the isotropic electronic polarizability, which is due to the zero-point (ZP) motion of the water molecule. In our case we obtain $\alpha_{el}^{ZP} = 0.2986$ a.u., in very good agreement with analogous calculations in the literature.[10,44]

The actual values for the electronic polarizability contribution to the first virial coefficient of water are reported in Table I and Fig. 1. We notice that our two calculation methods, PIMC and DVR, agree within mutual uncertainties at all the temperatures investigated in the present work. The PIMC approach is relatively noisy, but the DVR calculations clearly show that the electronic polarizability is a slightly increasing function of the temperature, exceeding its ground-state value by ~ 0.04% at $T = 100$ K. Unfortunately, we are not aware of any characterization of the uncertainty associated with the electronic polarizability surface[10] and hence we cannot provide a precise quantitative assessment of the uncertainty of $A_\varepsilon^{(el)}$.

These results for $A_\varepsilon^{(el)}$ can be compared to optical measurements of the refractivity of water vapor. The two most precise studies of this quantity were performed by Schödel et al.[11] and by Egan.[12] In order to compare with our static values of $A_\varepsilon^{(el)}$, the results must be adjusted to zero frequency; this can be done with the dipole oscillator strength sums of Zeiss and Meath.[43] The result-

TABLE I. The values of the electronic polarizability contribution to A_ε for $H_2{}^{16}O$. All of the uncertainties are reported at $k = 2$ coverage and do not include the propagation of the unknown uncertainty of the water electronic polarizability surface.

Temperature (K)	$A_\varepsilon^{(el)}$ (path-integral) (cm^3/mol)	$A_\varepsilon^{(el)}$ (DVR) (cm^3/mol)
1	–	3.67777 ± 0.00001
10	–	3.67786 ± 0.00007
25	–	3.67814 ± 0.00016
50	3.677 ± 0.001	3.67845 ± 0.00014
75	3.678 ± 0.001	3.67880 ± 0.00013
100	3.678 ± 0.001	3.67915 ± 0.00002
125	3.678 ± 0.001	3.6795 ± 0.0010
150	3.679 ± 0.002	3.680 ± 0.002
175	3.680 ± 0.002	3.680 ± 0.005
200	3.680 ± 0.003	3.681 ± 0.008
225	3.680 ± 0.003	3.681 ± 0.012
250	3.681 ± 0.003	3.681 ± 0.016
273.16	3.682 ± 0.004	3.68 ± 0.02
293.15	3.683 ± 0.004	3.68 ± 0.02
300	3.682 ± 0.004	3.68 ± 0.02
325	3.682 ± 0.004	3.68 ± 0.02
350	3.682 ± 0.005	3.68 ± 0.03
375	3.681 ± 0.006	3.68 ± 0.03
400	3.683 ± 0.007	3.68 ± 0.04
450	3.688 ± 0.007	3.68 ± 0.04
500	3.685 ± 0.007	3.69 ± 0.04
550	3.688 ± 0.008	–
600	3.68 ± 0.01	–
650	3.69 ± 0.01	–
700	3.69 ± 0.01	–
750	3.69 ± 0.01	–
800	3.69 ± 0.02	–
900	3.69 ± 0.02	–
1000	3.70 ± 0.02	–
1250	3.70 ± 0.03	–
1500	3.72 ± 0.04	–
1750	3.71 ± 0.04	–
2000	3.74 ± 0.06	–

ing values (at 293.15 K in both cases) are approximately 3.67 cm^3/mol, with expanded uncertainties on the order of 0.5%. This is in reasonable agreement with the values calculated here, although the comparison suggests that the polarizability surface of Lao et al.[10] may yield polarizabilities that are slightly too large (another possibility is inaccuracy in the dipole oscillator strengths of Ref. 43).

We also developed a correlation for $A_\varepsilon^{(el)}$ by fitting the numerical data using a function of the form

$$A_\varepsilon^{(el)}(T) = a_1 + \frac{a_2 T}{1 + \exp\left[-(T - a_3)/T_0\right]}. \quad (33)$$

The values of the fitted parameters a_i in Eq. (33) for the water isotopologues reported in this study are reported in Table II. The correlation reproduces the values reported in Table I within the assigned uncertainties in the temperature range between 1 and 2000 K.

TABLE II. Values of the parameters in Eq. (33) for the water isotopologues studied in this paper. The parameter T_0 has been set to 1 K.

Isotopologue	a_1 $(cm^3/(mol\ K))$	$a_2/10^{-5}$ $(cm^3/(mol\ K))$	a_3 (K)
$H_2^{16}O$	3.67777	1.38466	8.84684
$HD^{16}O$	3.66227	1.3733	9.63151
$D_2^{16}O$	3.6466	1.39401	5.3719

B. Dipolar polarizability

In order to discuss the dipolar contribution to the first dielectric virial coefficient, which is reported in Table III for various water models, let us begin by considering a classical rigid model (cf. Eq. (7)). The most striking difference with respect to the electronic polarizability contribution is the explicit appearance of a dependence on the inverse of the temperature. As a consequence, the values of $A_\varepsilon^{(dip)}$ cover a significantly larger range than those of $A_\varepsilon^{(el)}$. Therefore, we will plot the product of $A_\varepsilon^{(dip)}$ and the temperature T.

Using the same water geometry as before,[19] the dipole moment evaluated using the latest surface[10] would provide a value $\mu = 1.860$ D (1 D $\approx 3.33564 \times 10^{-30}$ C m); the square root of the average value of the dipole moment squared on the ground state of water is $\sqrt{\langle|\mathbf{m}|^2\rangle} = 1.857$ D using the same model. However, the smallness of the moments of inertia of water makes quantum rotational effects sizable; these can be investigated either with the semiclassical correction of Eq. (8) or with the more accurate path-integral simulation for rigid rotors described in Sec. IV B 1.

We report in Fig. 2 and Table III the values of the dipolar contribution to A_ε for several water models. The semiclassical approach and quantum rigid approach are in very good agreement for temperatures $T \gtrsim 100$ K. Additionally, quantum rotational effects are already appreciable at room temperature, where they contribute to a reduction of the dielectric virial coefficient by $\sim 3\%$ with respect to a classical value. Quantum rotational effects become progressively more important at lower temperatures, resulting in a reduction of $\sim 10\%$ at 100 K and $\sim 20\%$ at 50 K. The results of rigid-model PIMC calculations are in perfect agreement with the results obtained by diagonalization of the Hamiltonian of Eq. (32).

Figure 2 also shows the effect of molecular flexibility in determining $A_\varepsilon^{(dip)}$, as well as presenting the experimental values derived from the HITRAN2020 database. In general, the addition of flexibility results in a reduction of the dipolar contribution to the first dielectric virial coefficient, which is particularly evident at $T \leq 150$ K. The path-integral calculations are in very good agreement with values derived from spectroscopy, falling well within the estimated experimental uncertainty. We emphasize that we are not aware of any uncertainty estimates for the electronic-polarizability or dipole-moment surfaces,
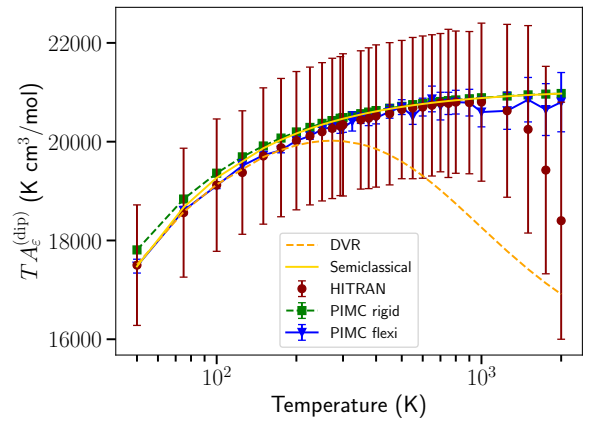

FIG. 2. The dipolar contribution to A_ε, $A_\varepsilon^{(dip)}$, multiplied by the temperature T of $H_2^{16}O$ as a function of temperature. Red circles: values and uncertainties obtained from HITRAN2020 data. Green squares: values obtained using a rigid quantum mechanical model. Blue triangles: values obtained using a flexible quantum mechanical model solved using PIMC. Dashed orange line: values obtained using a flexible quantum mechanical model, solved using DVR (the discrepancies for $T > 300$ K are due to insufficient convergence in the calculation of angular momentum states). Solid gold line: semiclassical values from Eq. (8). All theoretical uncertainties are reported at the $k = 2$ coverage value and do not include the propagation of the unknown uncertainty of the water dipole-moment surface. The lines joining the symbols are a guide to the eye. Error bars smaller than symbol sizes are not shown.

so we cannot provide a rigorous uncertainty analysis on A_ε at present and only its statistical contribution is reported. For the sake of a meaningful comparison, we collected enough statistics in the Monte Carlo calculations to make the statistical uncertainty smaller than the experimental one. The average values of our simulations and those computed from HITRAN2020 are in very good agreement at all the temperatures studied.

The computed and experimental values of $A_\varepsilon^{(dip)}$ begin to differ at high temperature; this is evident for $T \geq 1500$ K in the case of $H_2^{16}O$ and at even smaller temperatures for other isotopologues (as shown in Figures 2 and 5 of the Supplementary Material). We think that this discrepancy is due to the limited coverage of high-energy rovibrational states in the HITRAN2020 database, which limits the accuracy of the deduced values of $A_\varepsilon^{(dip)}$ at high temperatures.

Figure 2 also reports the calculation of $A_\varepsilon^{(dip)}$ performed using the DVR approach. The agreement with the path-integral calculation and with HITRAN2020 data is very good at temperatures $T \lesssim 300$ K. For higher temperatures, the DVR approach suffers from the limited number of angular momentum states J that we have been able to compute, and therefore the DVR values diverge from those obtained using PIMC. We note in passing that state-of-the-art rovibrational calculations of water up to

TABLE III. The values of the dipolar contribution to A_ε for $H_2{}^{16}O$ using various models, and its total value (last column) from path-integral simulations. All of the uncertainties are reported at $k = 2$ coverage and do not include the propagation of the unknown uncertainty of the water dipole-moment surface and potential-energy surface. A breakdown of the rotational and vibrational contributions to $A_\varepsilon^{(\mathrm{dip})}$ for H_2O is reported in Table I of the Supplementary Material.

Temperature (K)	$A_\varepsilon^{(\mathrm{dip})}$ (semiclassical) ($\mathrm{cm}^3/\mathrm{mol}$)	$A_\varepsilon^{(\mathrm{dip})}$ (HITRAN2020) ($\mathrm{cm}^3/\mathrm{mol}$)	$A_\varepsilon^{(\mathrm{dip})}$ (rigid) ($\mathrm{cm}^3/\mathrm{mol}$)	$A_\varepsilon^{(\mathrm{dip})}$ (flexible) ($\mathrm{cm}^3/\mathrm{mol}$)	A_ε (flexible) ($\mathrm{cm}^3/\mathrm{mol}$)
50	349.494	350 ± 12	356.2 ± 0.4	350 ± 6	353 ± 6
75	248.944	248 ± 9	251.18 ± 0.12	248 ± 2	252 ± 2
100	192.688	191 ± 7	193.62 ± 0.07	191.1 ± 1.3	194.8 ± 1.3
125	157.021	155 ± 5	157.54 ± 0.05	156.1 ± 1.0	159.7 ± 1.0
150	132.445	131 ± 5	132.75 ± 0.03	131.5 ± 0.7	135.2 ± 0.7
175	114.501	114 ± 4	114.70 ± 0.02	113.3 ± 0.6	117.0 ± 0.6
200	100.829	100 ± 4	100.985 ± 0.015	100.1 ± 0.6	103.8 ± 0.6
225	90.069	89 ± 3	90.173 ± 0.013	89.4 ± 0.6	93.1 ± 0.6
250	81.381	81 ± 3	81.482 ± 0.010	81.0 ± 0.6	84.7 ± 0.6
273.16	74.704	74 ± 3	74.779 ± 0.009	74.3 ± 0.6	78.0 ± 0.6
293.15	69.763	69 ± 2	69.833 ± 0.008	69.1 ± 0.6	72.8 ± 0.6
300	68.216	68 ± 2	68.290 ± 0.007	67.6 ± 0.6	71.3 ± 0.6
325	63.110	63 ± 2	63.162 ± 0.006	62.8 ± 0.6	66.5 ± 0.6
350	58.715	58 ± 2	58.761 ± 0.005	58.5 ± 0.6	62.2 ± 0.6
375	54.892	55 ± 2	54.931 ± 0.005	54.5 ± 0.6	58.2 ± 0.6
400	51.536	51 ± 2	51.575 ± 0.004	51.2 ± 0.6	54.9 ± 0.6
450	45.920	46 ± 2	45.951 ± 0.003	45.8 ± 0.5	49.5 ± 0.5
500	41.408	41.3 ± 1.4	41.431 ± 0.003	41.4 ± 0.7	45.1 ± 0.7
550	37.703	37.6 ± 1.3	37.726 ± 0.002	37.3 ± 0.6	41.0 ± 0.6
600	34.606	34.5 ± 1.2	34.6220 ± 0.0018	34.5 ± 0.7	38.2 ± 0.7
650	31.980	31.9 ± 1.1	31.9963 ± 0.0016	32.1 ± 0.8	35.8 ± 0.8
700	29.724	29.7 ± 1.0	29.7340 ± 0.0014	29.6 ± 0.7	33.3 ± 0.7
750	27.765	27.7 ± 1.0	27.7743 ± 0.0011	27.7 ± 0.6	31.4 ± 0.6
800	26.048	26.0 ± 0.9	26.0568 ± 0.0010	26.0 ± 0.7	29.7 ± 0.7
900	23.182	23.1 ± 0.8	23.1874 ± 0.0008	23.1 ± 0.7	26.9 ± 0.7
1000	20.884	20.8 ± 0.8	20.8891 ± 0.0006	20.6 ± 0.6	24.3 ± 0.6
1250	16.736	16.5 ± 0.7	16.7398 ± 0.0004	16.5 ± 0.7	20.2 ± 0.7
1500	13.962	13.5 ± 0.7	13.9650 ± 0.0003	13.9 ± 0.6	17.6 ± 0.6
1750	11.977	11.1 ± 0.6	11.9789 ± 0.0002	11.8 ± 0.5	15.6 ± 0.5
2000	10.487	9.2 ± 0.6	10.48780 ± 0.00016	10.4 ± 0.6	14.1 ± 0.6

$J = 72$ are available,[45] and therefore the DVR approach could be extended to higher temperatures.

The last column of Table III reports our theoretical estimate for the first dielectric virial coefficient of water, which has been obtained by summing the value of the dipolar contribution obtained using a flexible model of water (next-to-last column of the same table) and the electronic contribution reported in Table I.

Finally, we have also fitted the values of $A_\varepsilon^{(\mathrm{dip})}(T)$ computed using PIMC to a correlation of the form

$$A_\varepsilon^{(\mathrm{dip})}(T) = \frac{b_1(1 + b_4/T)/T}{1 + \exp\left[-(T - b_2)/b_3\right]}. \tag{34}$$

Values of the parameters b_i in Eq. (34) are reported in Table IV. The correlation reproduces the values reported in Table III within the assigned uncertainties in the temperature range between 50 and 2000 K.

C. Vibrational polarizability

Because the HITRAN2020 database allows us to distinguish between vibrational transitions and those in which only the rotational quantum numbers change, we can separate the calculated $A_\varepsilon^{(\mathrm{dip})}$ into vibrational and rotational parts. The detailed results for $H_2{}^{16}O$, $HD^{16}O$, and $D_2{}^{16}O$ are given in the Supplementary Material. The rotational contribution $\left(A_\varepsilon^{(\mathrm{dip,rot})}\right)$ is larger than the vibrational contribution $\left(A_\varepsilon^{(\mathrm{dip,vib})}\right)$ by roughly a factor of 600 at 300 K; our computed $A_\varepsilon^{(\mathrm{dip,vib})}$ have a small temperature dependence and for $H_2{}^{16}O$ have values slightly above 0.10 $\mathrm{cm}^3/\mathrm{mol}$ at typical temperatures of experimental interest (see Fig. 3).

The vibrational contribution to $A_\varepsilon^{(\mathrm{dip})}$ can be related to the molecule's vibrational polarizability, α_{vib}, by

$$A_\varepsilon^{(\mathrm{dip,vib})} = \frac{4\pi}{3} N_A \alpha_{\mathrm{vib}}. \tag{35}$$

Our calculations produce α_{vib} whose magnitude is

TABLE IV. Values of the parameters in Eqs. (34) and (37) for the water isotopologues studied in this paper.

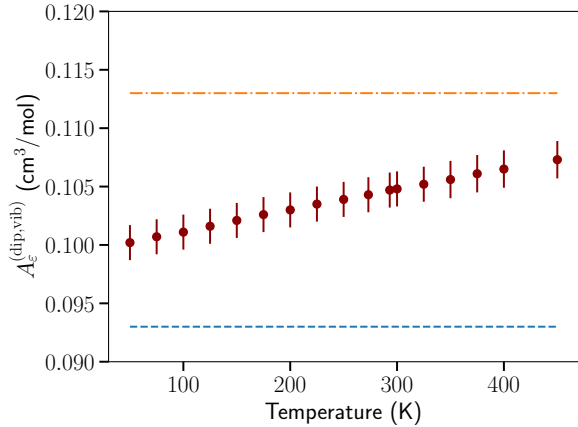| Isotopologue	b_1 (K cm^3/mol)	b_2 (K)	b_3 (K)	b_4 (K^2 cm^3/mol)
$H_2{}^{16}O$	20945.9	−693.079	184.074	−7.46202
$HD{}^{16}O$	21950.5	−11979.3	4072.31	−6.30806
$D_2{}^{16}O$	23949.4	−17378.8	9154.42	−4.5188

FIG. 3. The vibrational polarizability contribution to A_ε, $A_\varepsilon^{(\mathrm{dip,vib})}$, of $H_2{}^{16}O$ as a function of temperature, computed from spectroscopic information in the HITRAN2020 database.[23] The blue dashed line is the value 0.093 cm^3/mol calculated from a more crude use of spectroscopic data by Bishop and Cheung.[46] The orange dot-dashed line is the value 0.113 cm^3/mol from the *ab initio* calculations of Ruud *et al.*[47]

FIG. 4. The average dipole moment of $H_2{}^{16}O$ from our DVR (solid line) and PIMC (points) calculations. The shaded area denotes an estimate of the uncertainty of the DVR calculation. The PIMC error bars represent the expanded ($k = 2$) statistical uncertainty of the Monte Carlo calculation. The dashed line reports the experimental ground-state value of 1.85498 D from Ref. 13.

roughly 3% of the magnitude of the electronic polarizability; this is often considered an additional contribution when compiling the static polarizabilities of molecules.[48]

The vibrational polarizability has been a subject of some study, allowing comparison to previous estimates. Bishop and Cheung[46] estimated α_{vib} for H_2O and HDO based on the positions and integrated intensities of the three primary vibrational bands of the ground state. This can be thought of as an approximation to Eq. (25) in which each vibrational band is lumped into one line. Ruud *et al.*[47] estimated α_{vib} from *ab initio* calculations of a perturbation expansion of each normal vibration. The values of $A_\varepsilon^{(\mathrm{dip,vib})}$ derived from Refs. 46 and 47 for H_2O are 0.093 cm^3/mol and 0.113 cm^3/mol, respectively. These literature estimates are in reasonable agreement with our results, as shown in Fig. 3.

Bishop and Cheung made a similar estimate for the HDO molecule, producing $A_\varepsilon^{(\mathrm{dip,vib})} = 0.107$ cm^3/mol, which underestimates the vibrational polarizability (see Table IV in the Supplementary Material) by an amount somewhat less than that shown in Fig. 3 for H_2O.
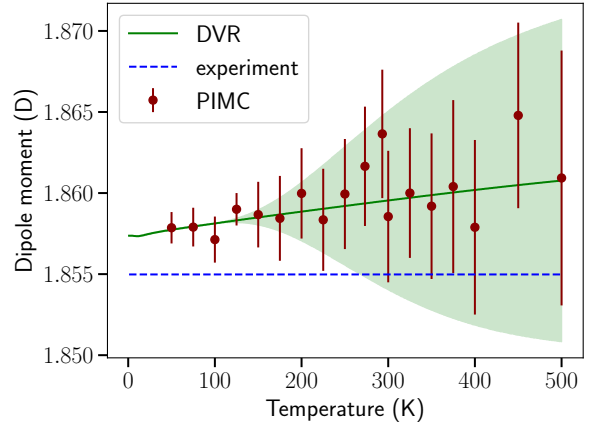
D. Dipole moment

We also computed the temperature-dependent value of the average dipole moment, defined as

$$\mu(T) = \sqrt{\sum_{J\nu} \frac{g_{J\nu}(2J+1)e^{-\beta E_{J\nu}}}{Q_1(\beta,0)} \langle \psi_{J\nu} \| \mathbf{m}|^2 | \psi_{J\nu} \rangle}, \quad (36)$$

where, as above, J and ν are the total angular momentum and vibrational quantum numbers of the water molecule and $g_{J\nu}$ is the degeneracy of these states. The results are reported in Fig. 4, where we also plot the experimental ground-state value of μ.[13] Similarly to what has been observed above, the PIMC calculations are rather noisy, but agree with the DVR results up to the highest temperature that we have investigated. We also report an estimate of the uncertainty of our DVR calculations, which is mainly due to the finite number of angular momentum states J considered in this work. A slight increase of the dipole moment with temperature is apparent in both cases (on the order of 0.2% from 0 K to 500 K), although the trend is probably clearer from the DVR results.

The value of the dipole moment at 0 K is that in the ground rovibrational state. The DVR calculations yield a dipole moment of 1.8574 D for $H_2{}^{16}O$, which is about

0.13% larger than the highly accurate ground-state value of 1.85498(9) D measured by Shostak *et al.*[13] A similar calculation for $D_2{}^{16}O$ yields a ground-state dipole moment of 1.8565 D, which exceeds by approximately 0.11% the experimental value of 1.8545(4) D measured by Dyke and Muenter.[49] These two comparisons with high-accuracy experimental results suggest that the dipole-moment surface we used,[27] which was designed more for spectroscopic applications than for accurate values of the dipole moment itself, is slightly biased toward high values.

E. Rescaled dipolar polarizability

The slightly too large dipole moments discussed in the previous section will result in a slightly overestimated dipolar polarizability. This can, however, be corrected in a straightforward manner because all contributions to the dipolar polarizability are proportional to the square of the dipole moment. We can therefore produce an improved estimate of the dipolar polarizability by multiplying Eq. (34) by the square of the ratio of the true ground-state dipole moment to that obtained here; for that purpose we use the H_2O value since it is the most accurately measured, producing a factor of $(1.85498/1.8574)^2 \approx 0.9974$. The rescaled dipolar polarizability is therefore given by

$$A_\varepsilon^{(\mathrm{dip,r})}(T) = 0.9974 \frac{b_1(1 + b_4/T)/T}{1 + \exp\left[-(T - b_2)/b_3\right]}, \quad (37)$$

with the parameters b_i given in Table IV. Equation (37) is valid in the temperature range between 50 and 2000 K. At all temperatures, the magnitude of this correction is smaller than the standard statistical uncertainty of the calculation of $A_\varepsilon^{(\mathrm{dip})}$.

VII. CONCLUSIONS

This work has presented the first complete theoretical calculation of water's first dielectric virial coefficient, A_ε, taking into account the flexibility of the water molecule and state-of-the-art descriptions of the variation of the electronic polarizability and the dipole moment with molecular geometry. The path-integral method, and in some cases the DVR approach to the three-body Hamiltonian, are used to perform the calculations with full accounting for quantum effects.

The contribution of the electronic polarizability to A_ε is not constant as is typically assumed, but increases slightly with temperature due to the different polarizabilities of states other than the rovibrational ground state. Our results are consistent with the best experimental values for this quantity, which are obtained from measurements of the refractive index.[11,12]

TABLE V. The values of the average dipole moment $\mu(T)$ of $H_2{}^{16}O$ (Debye) from Eq. (36) The PIMC uncertainties represent the expanded ($k = 2$) statistical uncertainty of the Monte Carlo calculation. Uncertainties do not include the propagation of the unknown uncertainty of the water dipole-moment surface.

Temperature (K)	$\mu(T)$ (PIMC) (D)	$\mu(T)$ (DVR) (D)
1	–	1.85737 ± 0.00001
10	–	1.85734 ± 0.00002
25	–	1.85749 ± 0.00004
50	1.858 ± 0.001	1.85774 ± 0.00003
75	1.858 ± 0.001	1.85794 ± 0.00003
100	1.857 ± 0.001	1.85813 ± 0.00010
125	1.859 ± 0.001	1.8583 ± 0.0003
150	1.859 ± 0.002	1.8585 ± 0.0005
175	1.858 ± 0.003	1.8587 ± 0.0010
200	1.860 ± 0.003	1.859 ± 0.002
225	1.858 ± 0.003	1.859 ± 0.003
250	1.860 ± 0.003	1.859 ± 0.004
273.16	1.862 ± 0.004	1.859 ± 0.005
293.15	1.864 ± 0.004	1.860 ± 0.005
300	1.859 ± 0.004	1.860 ± 0.006
325	1.860 ± 0.004	1.860 ± 0.006
350	1.859 ± 0.004	1.860 ± 0.007
375	1.860 ± 0.005	1.860 ± 0.008
400	1.858 ± 0.005	1.860 ± 0.008
450	1.865 ± 0.006	1.860 ± 0.009
500	1.861 ± 0.008	1.861 ± 0.010
600	1.858 ± 0.009	–
650	1.855 ± 0.009	–
700	1.873 ± 0.011	–
750	1.861 ± 0.012	–
800	1.858 ± 0.013	–
900	1.864 ± 0.013	–
1000	1.868 ± 0.014	–
1250	1.863 ± 0.017	–
1500	1.870 ± 0.020	–
1750	1.868 ± 0.021	–
2000	1.870 ± 0.025	–

The contribution of the dipolar polarizability also differs somewhat from the classical $\frac{\mu^2}{3k_\mathrm{B}T}$ functional form, both because values of the dipole moment other than the ground-state value are sampled at finite temperature and because of the quantization of rotation. The latter effect reduces the dipolar contribution to A_ε by roughly 3% at room temperature. The calculated dipolar contribution to A_ε also agrees well with estimates using line positions and intensities in the HITRAN2020 database.

In addition to the dominant isotopologue $H_2{}^{16}O$, we performed calculations for $D_2{}^{16}O$ and $HD{}^{16}O$. The data are presented in the Supplementary Material, but we note here that there is nothing surprising in the results. The electronic polarizability (and therefore $A_\varepsilon^{(\mathrm{el})}$) is smaller by amounts on the order of 0.5% for $HD{}^{16}O$ and 1% for $D_2{}^{16}O$. This probably reflects the shorter average length of O–D bonds compared to O–H bonds. The dipole moment is slightly reduced by D substitution, in agreement

with the experimental result for $D_2{}^{16}O$.[49] The dipolar contribution $A_\varepsilon^{(\mathrm{dip})}$ is not affected (within the uncertainty of our calculations) by D substitution at high temperatures. However, below about 500 K, D substitution noticeably increases $A_\varepsilon^{(\mathrm{dip})}$. This is because the substitution increases the moment of inertia, reducing the magnitude of the (negative) correction to $A_\varepsilon^{(\mathrm{dip})}$ due to the quantization of rotation [expressed semiclassically by Eq. (8)].

Our results for A_ε provide accurate, temperature-dependent data that can be used to describe the effect of water on the static dielectric constant of gases for humidity metrology. They can also serve as a low-density boundary condition for future comprehensive formulations for the static dielectric constant of H_2O and D_2O. We note that the current international standard formulation for the dielectric constant of H_2O[6,7] does not account for the quantum effects studied in this work; it also uses a dipole moment that is roughly 1% smaller than the best experimental value,[13] which in our terminology produces a value of $A_\varepsilon^{(\mathrm{dip})}$ that is roughly 2% too small. Our results for $A_\varepsilon^{(\mathrm{el})}$ could also be used to improve the standard formulation for the refractive index of water,[7,50] although this would require a dispersion correction from our static values to optical frequencies.

Our recommended formula for $A_\varepsilon(T)$ is given by

$$A_\varepsilon(T) = A_\varepsilon^{(\mathrm{el})}(T) + A_\varepsilon^{(\mathrm{dip,r})}(T), \qquad (38)$$

where the electronic polarizability contribution $A_\varepsilon^{(\mathrm{el})}$ is given by Eq. (33) and the (rescaled) dipolar contribution $A_\varepsilon^{(\mathrm{dip,r})}$ is given by Eq. (37). Similarly to Eq. (37), Eq. (38) is valid in the temperature range $50 - 2000$ K.

Extension beyond the low-density limit would require the second dielectric virial coefficient, B_ε. B_ε can be computed in a straightforward way for noble gases,[17] but the calculation is much more difficult for a molecule like water. The largest effect would likely come from the correlation of molecular dipoles due to the pair potential; this would be relatively straightforward for a rigid, non-polarizable model and Yang et al.[51] performed such a calculation for a simple water model. A complete calculation of B_ε would require a multidimensional surface for the nonadditive electronic polarizability and for changes in multipole moments as the molecules mutually polarize each other. Incorporating the flexibility of the molecules would greatly increase the complexity, and is likely impractical at present. A classical calculation of B_ε with a rigid, polarizable water model was performed by Stone et al.;[52] thus far the result has not been confirmed by independent calculations and unfortunately there seem to be no reliable experimental determinations of B_ε. Additional rigorous calculations of B_ε for water would therefore be desirable.

VIII. SUPPLEMENTARY MATERIAL

The Supplementary Material includes the following: derivation of Eqs. (9) and (10), a table with the breakdown of the vibrational and rotational contributions to $A_\varepsilon^{(\mathrm{dip})}$ for H_2O. Tables and figures reporting $A_\varepsilon^{(\mathrm{el})}$ and dipole moments of HDO and D_2O. Tables and figures reporting the computed $A_\varepsilon^{(\mathrm{dip})}$ for HDO and D_2O, their division into vibrational and rotational contributions, and their derivation from HITRAN2020 data

IX. ACKNOWLEDGMENTS

AUTHOR DECLARATIONS

Conflict of Interest

The authors have no conflicts to disclose.

DATA AVAILABILITY

The data that support the findings of this study are available within the article and its Supplementary Material.

Appendix A: Wavefunction expression for $\alpha_{\mathrm{dip}}(T)$

1. Flexible models

The derivation of the expression of $\alpha_{\mathrm{dip}}(T)$ starts from the general formula of Eq. (10) and the representation of the molecular quantum states of Eq. (19). In fact, the indices i and j in Eq. (10) stand for all the quantum numbers needed to describe a given molecular state, that is $i \equiv J\nu mI$. Correspondingly, we will indicate the quantum numbers corresponding to the index j with primed quantities, i.e., $j \equiv J'\nu'm'I'$. Since energies depend only on the quantum numbers J and ν, and since the matrix element of the dipole moment operator does not act on the nuclear spins, one can perform the sum over I and I' obtaining

$$\sum_{I,I'} \left| \chi^*(\mathcal{I}_{J\nu}, I)\chi(\mathcal{I}_{J'\nu'}, I') \right|^2 = g_{J\nu}\delta_{g_{J\nu}, g_{J'\nu'}}, \qquad (\mathrm{A1})$$

that is, the sum over the nuclear spin states allows only ortho-ortho or para-para transitions, and provides the corresponding degeneracy factor.

Additionally, particular care must be taken to evaluate the matrix element of $\mathbf{m}\cdot\mathbf{e}$, where we will assume, without loss of generality, that we are considering $\mathbf{e}$ aligned along the Z axis in the laboratory frame. However, the DVR procedure writes the wavefunction with coordinates q that are defined in the so-called molecular frame, where the orientation of the molecule is fixed. In order to evaluate the matrix elements of $\mathbf{m}_Z$, one has to recall that it transforms as the 0-th component of a vector operator, which means that it is given by[18,32,35]

$$\mathbf{m}_0^{\mathrm{L}} = \sum_{K=1}^{1} \mathbf{m}_K^{\mathrm{M}}(q) D_{0K}^{1*}(\Omega), \tag{A2}$$

where the superscript 'L' denotes the spherical compo-

nents of the operator in the laboratory-fixed frame, and the superscript 'M' denotes spherical components in the molecule-fixed frame. Using the identities

$$\int D_{m_1 k_1}^{J_1}(\Omega) D_{m_2 k_2}^{J_2}(\Omega) D_{m_3 k_3}^{J_3}(\Omega)\mathrm{d}\Omega =$$
$$8\pi^2 \begin{pmatrix} J_1 & J_2 & J_3 \\ m_1 & m_2 & m_3 \end{pmatrix}\begin{pmatrix} J_1 & J_2 & J_3 \\ k_1 & k_2 & k_3 \end{pmatrix} \tag{A3}$$

$$\sum_{mm'} \begin{pmatrix} J' & 1 & J \\ m' & 0 & m \end{pmatrix} = \frac{1}{3} \tag{A4}$$

one arrives from Eq. (10) to

$$\alpha_{\mathrm{dip}}(T) = \sum_{J'\nu',J\nu} \frac{(2J'+1)(2J+1)}{3} \left| \sum_{k'=k-1,k}^{k+1,\infty} \langle \psi_{J'\nu'k'} | \mathbf{m}_{k'-k}^{\mathrm{M}} | \psi_{J\nu k}\rangle (-1)^{k'} \begin{pmatrix} J' & 1 & J \\ -k' & k'-k & k \end{pmatrix} \right|^2 g_{J\nu}\delta_{g_{J\nu},g_{J'\nu'}} \frac{\mathrm{e}^{-\beta E_{J'\nu'}} - \mathrm{e}^{-\beta E_{J\nu}}}{E_{J\nu} - E_{J'\nu'}}, \tag{A5}$$

where, in the DVR approach, one has

$$\langle \psi_{J'\nu'k'} | \mathbf{m}_{k'-k}^{\mathrm{M}} | \psi_{J\nu k}\rangle = \sum_q \psi_{J'\nu'k'}(q) \mathbf{m}_{k'-k}^{\mathrm{M}}(q) \psi_{J\nu k}(q) \tag{A6}$$

since the spherical components of the dipole-moment operator are diagonal in the molecule-fixed frame. In Eq. (A5), the quantity $\begin{pmatrix} J' & 1 & J \\ -k' & k'-k & k \end{pmatrix}$ is a Wigner $3j$-symbol. The diagonalization procedure outlined in Sec. IV A provides, for any given angular momentum J, the energies $E_{J\nu}$ and the wavefunctions $\psi_{J\nu k}(q)$ (as the eigenvalues and eigenvectors of the three-body Hamiltonian in the molecule-fixed frame, respectively), enabling a straightforward evaluation of the dipolar polarizability using Eqs. (A6) and (A5). In this paper, we obtained the degeneracy factors $g_{J\nu}$ from the HITRAN2020 database.

2. Rigid models

Equation (A5) is valid also in the case of rigid molecular models of water. In this case, the eigenfunctions do not depend on the coordinates q describing the molecular vibrations, so that the matrix element of Eq. (A6) is replaced by

$$\langle \psi_{J'\nu'k'} | \mathbf{m}_{k'-k}^{\mathrm{M}} | \psi_{J\nu k}\rangle = \psi_{J'\nu'k'} \mathbf{m}_{k'-k}^{\mathrm{M}} \psi_{J\nu k} \tag{A7}$$

where now $\psi_{J\nu k}$ are the eigenfunctions of the rigid-rotor Hamiltonian (see Sec. V A 2). In the case of a rigid molecule, the matrix elements of the spherical components of the dipole-moment operator, $\mathbf{m}_{k'-k}^{\mathrm{M}}$, are constants.

[1] P. H. Huang, D. C. Ripple, M. R. Moldover, and G. E. Scace, "Re-entrant radio-frequency resonator hygrometer for fuel cell research and development," in *Proceedings, 2005 Fuel Cell Seminar* (Palm Springs, CA, 2005).

[2] P. H. Huang, D. C. Ripple, M. R. Moldover, and G. E. Scace, "A reference standard for measuring humidity of air using a re-entrant radio frequency resonator," in *Proceedings of the 5th International Symposium on Humidity and Moisture* (Rio de Janeiro, Brazil, 2006).

[3] D. Vega-Maza, W. W. Miller, D. C. Ripple, and G. E. Scace, "A humidity generator for temperatures up to 200 °C and pressures up to 1.6 MPa," Int. J. Thermophys. **33**, 1477 (2012).

[4] R. Cuccaro, R. M. Gavioso, G. Benedetto, D. Madonna Ripa, V. Fernicola, and C. Guianvarc'h, "Microwave determination of water mole fraction in humid gas mixtures," Int. J. Thermophys. **33**, 1352 (2012).

[5] R. M. Gavioso, D. Madonna Ripa, R. Benyon, J. G. Gallegos, F. Perez-Sanz, S. Corbellini, S. Avila, and A. M. Benito, "Measuring humidity in methane and natural gas with a microwave technique," Int. J. Thermophys. **35**, 748 (2014).

[6] D. P. Fernández, A. R. H. Goodwin, E. W. Lemmon, J. M. H. Levelt Sengers, and R. C. Williams, "A formulation for the static permittivity of water and steam at temperatures from 238 K to 873 K at pressures up to 1200 MPa, including derivatives and Debye–Hückel coefficients," J. Phys. Chem. Ref. Data **26**, 1125–1166 (1997).

[7] A. H. Harvey, J. Hrubý, and K. Meier, "Improved and always improving: Reference formulations for thermophysical properties of water," J. Phys. Chem. Ref. Data **52**, 011501 (2023).

[8] J. K. Conrad, H. Arcis, J. P. Ferguson, and P. R. Tremaine, "Second ionization constant of sulfuric acid in H_2O and D_2O from 150 to 300 °C at $p = 11.5$ MPa using flow AC conductivity," Phys. Chem. Chem. Phys. **25**, 1659–1676 (2023).

[9] A. H. Harvey, P. R. Tremaine, J. S. Cox, and J. M. Young, "Developing a formulation for the static dielectric constant of D_2O," (2023), annual meeting of the International Association for the Properties of Water and Steam, Turin, Italy.

[10] K. U. Lao, J. Jia, R. Maitra, and R. A. DiStasio, "On the geometric dependence of the molecular dipole polarizability in water: A benchmark study of higher-order electron correlation, basis set incompleteness error, core electron effects, and zero-point vibrational contributions," J. Chem. Phys. **149**, 204303 (2018).

[11] R. Schödel, A. Walkov, and A. Abou-Zeid, "High-accuracy determination of water vapor refractivity by length interferometry," Opt. Lett. **31**, 1979 (2006).

[12] P. F. Egan, "Capability of commercial trackers as compensators for the absolute refractive index of air," Precision Eng. **77**, 46 (2022).

[13] S. L. Shostak, W. L. Ebenstein, and J. S. Muenter, "The dipole moment of water. I. Dipole moments and hyperfine properties of H_2O and HDO in the ground and excited vibrational states," J. Chem. Phys. **94**, 5875 (1991).

[14] T. B. MacRury and W. A. Steele, "Quantum effects on the dielectric virial coefficients of polar gases," J. Chem. Phys. **61**, 3352 (1974).

[15] C. G. Gray, K. E. Gubbins, and C. G. Joslin, *Theory of Molecular Fluids*, Vol. 2: Applications (Oxford Science Publications, 2011).

[16] T. L. Hill, "Theory of the dielectric constant of imperfect gases and dilute solutions," J. Chem. Phys. **28**, 61 (1958).

[17] G. Garberoglio, A. H. Harvey, and B. Jeziorski, "Path-integral calculation of the third dielectric virial coefficient of noble gases," J. Chem. Phys. **155**, 234103 (2021).

[18] R. N. Zare, *Angular Momentum: Understanding Spatial Aspects in Chemistry and Physics* (Wiley, New York, 1988).

[19] G. Czakó, E. Mátyus, and A. G. Császár, "Bridging theory with experiment: A benchmark study of thermally averaged structural and effective spectroscopic parameters of the water molecule," J. Phys. Chem. A **113**, 11665 (2009).

[20] K. H. Illinger and C. P. Smyth, "Atomic polarization. I. Vibrational polarization of gases," J. Chem. Phys. **32**, 787 (1960).

[21] D. M. Bishop, "Molecular vibrational and rotational motion in static and dynamic electric fields," Rev. Mod. Phys. **62**, 343 (1990).

[22] R. C. Hilborn, "Einstein coefficients, cross sections, f-values, dipole moments, and all that," Am. J. Phys. **50**, 982 (1982).

[23] I. E. Gordon *et al.*, "The HITRAN2020 molecular spectroscopic database," J. Quant. Spectrosc. Radiat. Trans. **277**, 107949 (2021).

[24] R. R. Gamache and L. S. Rothman, "Extension of the HITRAN database to non-LTE applications," J. Quant. Spectrosc. Radiat. Trans. **48**, 519 (1992).

[25] M. Šimečková, D. Jacquemart, L. S. Rothman, R. R. Gamache, and A. Goldman, "Einstein A-coefficients and statistical weights for molecular absorption transitions in the HITRAN database," J. Quant. Spectrosc. Radiat. Trans. **98**, 130 (2006).

[26] I. I. Mizus, A. A. Kyuberis, N. F. Zobov, V. Y. Makhnev, O. L. Polyansky, and J. Tennyson, "High-accuracy water potential energy surface for the calculation of infrared spectra," Phil. Trans. Royal Soc. A **376**, 20170149 (2018).

[27] E. K. Conway, A. A. Kyuberis, O. L. Polyansky, J. Tennyson, and N. F. Zobov, "A highly accurate ab initio dipole moment surface for the ground electronic state of water vapour for spectra extending into the ultraviolet," J. Chem. Phys. **149**, 084307 (2018).

[28] B. T. Sutcliffe and J. Tennyson, "Variational methods for the calculation of rovibrational energy levels of small molecules," J. Chem. Soc., Faraday Trans. 2 **83**, 1663 (1987).

[29] J. C. Light and T. Carrington Jr, "Discrete-variable representations and their utilization," Adv. Chem. Phys. **114**, 263 (2000).

[30] V. Szalay, "Discrete variable representations of differential operators," J. Chem. Phys. **99**, 1978 (1993).

[31] D. Baye, "The Lagrange-mesh method," Phys. Rep. **565**, 1 (2015).

[32] J. Tennyson, M. A. Kostin, P. Barletta, G. J. Harris, O. L. Polyansky, J. Ramanlal, and N. F. Zobov, "DVR3D: a program suite for the calculation of rotation–vibration spectra of triatomic molecules," Comput. Phys. Commun. **163**, 85 (2004).

[33] G. Czakó, T. Furtenbacher, A. G. Császár, and V. Szalay, "Variational vibrational calculations using high-order anharmonic force fields," Mol. Phys. **102**, 2411 (2004).

[34] E. Mátyus, C. Fábri, T. Szidarovszky, G. Czakó, W. D. Allen, and A. G. Császár, "Assigning quantum labels to variationally computed rotational-vibrational eigenstates of polyatomic molecules," J. Chem. Phys. **133**, 034113 (2010).

[35] C. R. Le Sueur, S. Miller, J. Tennyson, and B. T. Sutcliffe, "On the use of variational wavefunctions in calculating vibrational band intensities," Mol. Phys. **76**, 1147 (1992).

[36] R. P. Feynman and A. Hibbs, *Quantum Mechanics and Path Integrals* (McGraw-Hill, New York, 1965).

[37] E. G. Noya, L. M. Sesé, R. Ramírez, C. McBride, M. M. Conde, and C. Vega, "Path integral Monte Carlo simulations for rigid rotors and their application to water," Mol. Phys. **109**, 149 (2011).

[38] E. G. Noya, C. Vega, and C. McBride, "A quantum propagator for path-integral simulations of rigid molecules," J. Chem. Phys. **134**, 054117 (2011).

[39] G. Garberoglio, P. Jankowski, K. Szalewicz, and A. H. Harvey, "Fully quantum calculation of the second and third virial coefficients of water and its isotopologues from ab initio potentials," Faraday Discuss. **148**, 174501 (2018).

[40] D. M. Bishop, J. Pipin, and J. N. Silverman, "Methods for introducing vibrational effects in the calculation of electric dipole polarizabilities and hyperpolarizabilities (with reference to H_2^+)," Mol. Phys. **59**, 165 (1986).

[41] R. Hellmann and A. H. Harvey, "First-principles diffusivity ratios for kinetic isotope fractionation of water in air," Geophys. Res. Lett. **47**, e2020GL089999 (2020).

[42] M. E. Tuckerman, B. J. Berne, G. J. Martyna, and M. L. Klein, "Efficient molecular dynamics and hybrid Monte Carlo algorithms for path integrals," J. Chem. Phys. **99**, 2796 (1993).

[43] G. D. Zeiss and W. J. Meath, "Dispersion energy constants $C_6(A, B)$, dipole oscillator strength sums and refractivities for Li, N, O, H_2, N_2, O_2, NH_3, H_2O, NO and N_2O," Mol. Phys. **33**, 1155 (1977).

[44] G. Avila, "Ab initio dipole polarizability surfaces of water molecule: Static and dynamic at 514.5 nm," J. Chem. Phys. **122**, 144310 (2005).

[45] O. L. Polyansky, A. A. Kyuberis, N. F. Zobov, J. Tennyson, S. N. Yurchenko, and L. Lodi, "ExoMol molecular line lists XXX: a complete high-accuracy line list for water," Monthly Notices of the Royal Astronomical Society **480**, 2597–2608 (2018).

[46] D. M. Bishop and L. M. Cheung, "Vibrational contributions to molecular dipole polarizabilities," J. Phys. Chem. Ref. Data **11**, 119–133 (1982).

[47] K. Ruud, D. Jonsson, and P. R. Taylor, "Vibrational effects on electric and magnetic susceptibilities: application to the properties of the water molecule," Phys. Chem. Chem. Phys. **2**, 2161–2171 (2000).

[48] U. Hohm, "Experimental static dipole–dipole polarizabilities of molecules," J. Mol. Struct. **1054-1055**, 282–292 (2013).

[49] T. R. Dyke and J. S. Muenter, "Electric dipole moments of low J states of H_2O and D_2O," J. Chem. Phys. **59**, 3125 (1973).

[50] A. H. Harvey, J. S. Gallagher, and J. M. H. Levelt Sengers, "Revised Formulation for the Refractive Index of Water and Steam as a Function of Wavelength, Temperature and Density," J. Phys. Chem. Ref. Data **27**, 761 (1998).

[51] S. Yang, A. J. Schultz, and D. A. Kofke, "Evaluation of second and third dielectric virial coefficients for non-polarisable molecular models," Mol. Phys. **115**, 991 (2017).

[52] A. J. Stone, Y. Tantirungrotechai, and A. D. Buckingham, "The dielectric virial coefficient and model intermolecular potentials," Phys. Chem. Chem. Phys. **2**, 429 (2000).